Available online at www.sciencedirect.com
ScienceDirect
Trans. Nonferrous Met. Soc. China 35(2025) 1634−1647
Transactions of Nonferrous Metals Society of China
www.tnmsc.cn

Edge cracking behavior of copper foil in asymmetrical micro-rolling

Jing-qi CHEN[1,2], Lin-yun ZHENG[1,2], Wei ZHAO[1,2], Zhen-hua BAI[1,2], Xue-tong LI[1,2], Ri-huan LU[1,2], Shou-dong CHEN[3], Xiang-hua LIU[4], Hai-tao GAO[5], Hai-liang YU[5]

1. National Engineering Research Center for Equipment and Technology of Cold Rolled Strip, Yanshan University, Qinhuangdao 066004, China;
2. College of Mechanical Engineering, Yanshan University, Qinhuangdao 066004, China;
3. School of Mechanical Engineering, Tongling University, Tongling 244061, China;
4. School of Materials Science and Engineering, Northeastern University, Shenyang 110819, China;
5. School of Mechanical and Electrical Engineering, Central South University, Changsha 410083, China

Received 8 September 2023; accepted 11 May 2024

Abstract: The edge crack behavior of copper foil in asymmetrical micro-rolling was studied. The effects of the speed ratio between rolls, grain size and stress state in the deformation zone on edge cracks of the rolled piece in asymmetrical rolling were analyzed. Low plasticity, uneven deformation and longitudinal secondary tensile stress generated in the edge area of the rolled piece during the rolling process are the main causes of edge cracks. The larger the grain size of the rolled piece, the smaller the number of edge cracks and the deeper the expansion depth, and the larger the spacing between cracks under the same rolling reduction. Asymmetrical rolling can effectively increase the rolling reduction at when the copper foil fist shows edge cracks compared to symmetrical rolling. This enhancement is attributed to the shearing stress induced by asymmetrical rolling, which reduces the rolling force and longitudinal secondary tensile stress, and increases the residual compressive stress on the surface of the rolled piece. The edge crack defects of copper foil can be effectively reduced by increasing the speed ratio between the rolls in asymmetrical rolling.
Key words: edge crack; copper foil; asymmetrical rolling; size effect

1 Introduction

Copper foil, referred to as the “neural network” for electronic signal and power transmission, is highly valued for its superior processability and electrical conductivity [1−3]. Edge cracks, which frequently occur during the cold rolling process of copper foil, are characterized as fractures that manifest on one or both sides of the edge of the rolled piece. These defects propagate transversely during continuous rolling and are conventionally mitigated through edge trimming in industrial production. Notably, severe edge cracks may trigger catastrophic strip breakage during processing, resulting in substantial economic losses.

In recent years, extensive research has been conducted on edge cracking of various metals and their alloys during the rolling process. YAN et al [4] demonstrated that large-diameter work rolls are beneficial in reducing edge cracks in cold rolling deformation of silicon steel sheets. High surface roughness is considered to be an important cause for edge cracks during the rolling process of low-carbon steel with a thickness of 2 mm [5]. It is reported that the plastic damage is caused by the shear deformation and hole accumulation during the rolling process of Mg plates with a final rolling

Corresponding author: Jing-qi CHEN, Tel: +86-15940256519, E-mail: chenjq24@163.com;
Hai-liang YU, Tel: +86-18511635397, E-mail: yuhailiang@csu.edu.cn
https://doi.org/10.1016/S1003-6326(25)66772-0

thickness of 3 mm [6]. Systematic investigations of multifactorial edge crack origins have enabled the establishment of diversified ductile damage criteria for cold-rolled alloys. Impurities in the edge area of the rolled piece can easily cause strain localization during the rolling process, resulting in edge cracks [7]. Edge cracks in rolled pieces can be attributed to the longitudinal tensile stress in the edge region exceeding the theoretical fracture strength of the material [8]. LEE et al [9] found that edge drop promotes the generation of edge cracks in copper alloys rolling with a six-high mill. While these studies establish comprehensive frameworks for macroscale edge cracking phenomena, their applicability diminishes at microscale dimensions due to intrinsic size effects governing material fracture behavior.

Although numerous studies on the micro-rolling of copper foil have been conducted, most are confined to the rolling mechanics, with very few focusing on product quality, especially edge crack defects. WANG et al [10] proposed an idea of using the double rolling method to prepare the copper foil so that it has a sufficiently large matte surface roughness and meets the requirements for firm bonding with the resin substrate. CHEN et al [11] focused on the effect of grain size and heterogeneity on the mechanical behavior of foil rolling using a grain-level finite element analysis in combination with a rate-dependent crystal plasticity constitutive model. The existing researches on the edge cracking behavior of metal foil predominantly concentrate on the effect of the initial microstructure of rolled pieces on the subsequent edge cracking behavior. Mg foil with a thickness of 35 μm without edge cracks can be obtained by controlling the initial microstructure of the blank before rolling [12]. ZHAO et al [13] found that copper foils with grain sizes of 19 and 23 μm were free from edge cracks after a reduction of 70%.

The advantages of asymmetrical rolling in the preparation of metal foil have been gradually unveiled in recent years. WANG et al [14] developed a model based on the slab method to analyze the effects of mechanical parameters, including roll speed, roll diameter, friction coefficient, roll force, and roll torque in asymmetrical rolling. TANG et al [15,16] studied the permissible minimum thickness in asymmetrical cold strip rolling using the slab method. CHEN et al [17,18] improved the corrosion resistance of copper foil and the electrochemical performance of lithium-ion batteries by utilizing electrodeposited copper foil as the raw material through asymmetrical rolling and surface morphology modification. Asymmetrical rolling is recognized as an effective means to produce high-quality metal foil. However, the edge cracking behavior of metal foil in multi-pass asymmetrical micro-rolling remains systematically unexplored. In this work, the edge cracking behavior of copper foil in asymmetrical and symmetrical rolling is compared to explore the advantages of asymmetrical rolling to produce metal foil. Additionally, the influence of size effect on the edge cracking behavior of copper foil is analyzed, providing theoretical and practical guidance for producing metal foil by asymmetrical rolling.

2 Experimental

Copper foil with a thickness of 80 μm was annealed under conditions of (500 °C, 1 h), (600 °C, 2 h) and (950 °C, 2 h) to obtain different grain sizes for the uniaxial tensile test and asymmetrical micro-rolling test. Uniaxial tensile tests were performed on an Instron 5969 microforce Testing System (Illinois Tool Works Inc. Cincinnati, OH, USA) at room temperature. The tensile samples, fabricated in accordance with the ASTM E8/E8M—21 standard [19], were cut into dog bone-shaped specimens, each with a gauge length of 50 mm and a width of 12.5 mm. To ensure the precision of the results, each test was conducted at a loading rate of 1 mm/min and replicated five times. The surface and lateral roughnesses of the specimens were meticulously controlled, as these characteristics were recognized to significantly influence the stability of the uniaxial tensile test data. The surface quality of the samples was rigorously inspected to preclude any scratches or pits. During the electric discharge machining, the cutting speed was meticulously reduced to safeguard the specimen integrity. Furthermore, the cut surfaces of the samples were carefully abraded with 3000# sandpaper prior to the uniaxial tensile testing.

The asymmetrical micro-rolling experiment was performed on our self-developed metal micro-forming mill. The diameter of the work roll was

50 mm, the length of the roll body was 130 mm, and the speed of the two work rolls can be adjusted separately to obtain different speed ratios. Rectangular samples, measuring 50 mm by 20 mm, underwent rolling at these varied speed ratios to ascertain the edge cracking behavior. The initial thickness of copper foil prior to rolling was maintained at 80 μm, with the rolling force maintained within a range of 10−85 kN and the speed ratio between rolls varying from 1.0 to 1.3. The surface morphology of the samples was examined using a scanning electron microscope (SEM, Ultra 55, Zeiss, Oberkochen, Germany), and the residual compressive stress within the samples was quantified using X-ray diffraction (XRD, PANalytical BV, Almelo, Netherlands).

3 Results

3.1 Microstructure and mechanical properties

The microstructures of the samples, depicted in Fig. 1, exhibit the characteristic grain boundaries and twin boundaries typical of annealed copper. The grain size of the copper foil is observed to increase incrementally with increasing annealing temperatures and extended durations. The linear intercept method was employed to calculate the grain sizes of the as-received samples and those annealed at 500 °C for 1 h, 600 °C for 2 h, and 950 °C for 2 h, which were determined to be 3.3, 7.7, 23.2, and 75.2 μm, respectively. Concurrently, the ratio of sample thickness (T) to grain size (D), denoted as T/D, was diminished progressively with the escalation of grain size, exhibiting values of 24.2, 10.4, 3.4 and 1.1, respectively. The distribution of the various grain types was observed to be relatively uniform in the fine-grained samples; however, this uniformity was disrupted when the T/D ratio fell below 10. The shape, orientation, and deformation characteristics of individual grains were identified to exert a more pronounced impact on the overall deformation behavior of the copper foil. Particularly, when the T/D ratio approaches 1, the influence of the size effects on the deformation of the copper foil becomes markedly more significant.

Engineering stress−strain curves of copper foil with varying grain sizes are exhibited in Fig. 2. Figure 3 shows the variation of fracture stress and fracture strain with grain size. The mechanical properties of copper foil with different grain sizes were analyzed in detail in our previous work [20]. In brief, the fracture behavior of copper foil changed significantly with a decrease in the number of grains along the thickness direction. The quantity of dimples observed on the fracture surface was noted to diminish progressively with an increase in grain size. When the T/D ratio of copper foil was less than 10, dimples were not observed on the fracture surface, and both the fracture stress and strain decreased with the increase in grain size. The fracture process of the copper foil was determined to be intricately linked to the surface roughness. Variations in the degree of deformation and the presence of slip marks on the surface of different grains resulted in enhanced surface roughening during the tensile deformation process. The local depression and thinning of the sample caused by surface roughening occurred during the initial stage of tensile deformation, leading to the reduction of fracture stress and strain.

A transition from polycrystalline to single-crystal behavior occurs when the T/D ratio falls

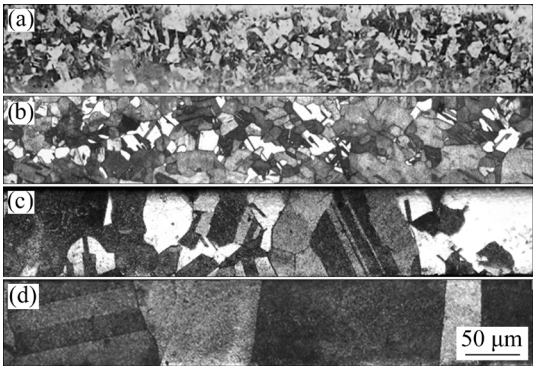

Fig. 1 Microstructures of samples with different grain sizes: (a) 3.3 μm; (b) 7.7 μm; (c) 23.2 μm; (d) 75.2 μm

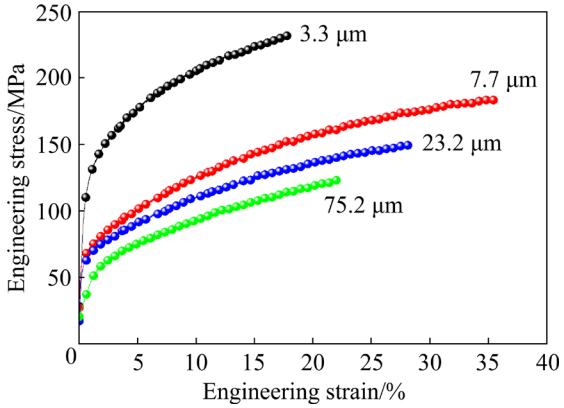

Fig. 2 Engineering stress−strain curves of copper foil with different grain sizes

below 10 [21]. In the context of tensile deformation, samples with a *T*/*D* ratio less than 10 exhibit deformation characteristics that are predominantly influenced by the properties of individual grains. In such instances, the coordination of deformation among adjacent grains is markedly compromised, leading to a non-uniform distribution of strain within the deformation zone. This results in the onset of strain localization at the initial stage of necking. Consequently, as the grain size increases, there is a discernible reduction in both the fracture stress and strain of the material, reflecting the altered deformation mechanisms at the micro-structural level.

3.2 Advantage of asymmetrical rolling

Figure 4 shows the relationship between rolling force and sample thickness during the initial nine passes of both symmetrical and asymmetrical rolling, at various speed ratios between the rolls. A pronounced reduction in the thickness of the rolled pieces is observed as the rolling force escalates from 10 to 22 kN. Nevertheless, as the rolling force progresses from 22 to 85 kN, the curves for both

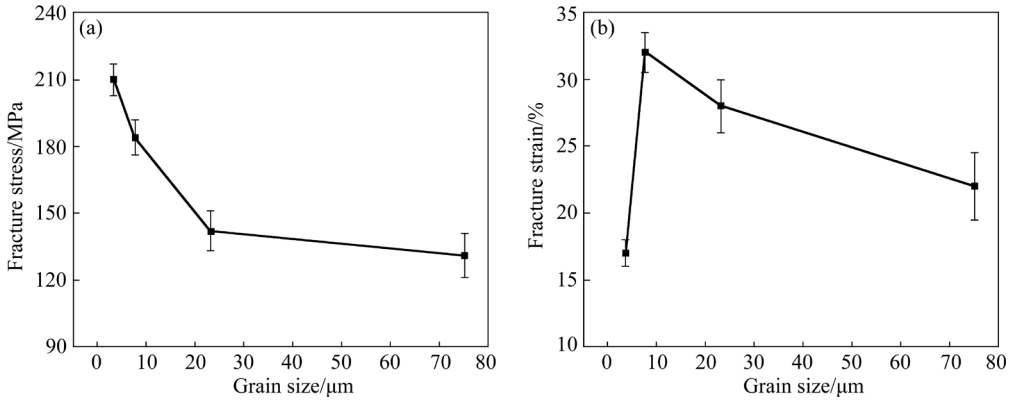

Fig. 3 Variation of fracture stress (a) and fracture strain (b) with grain size

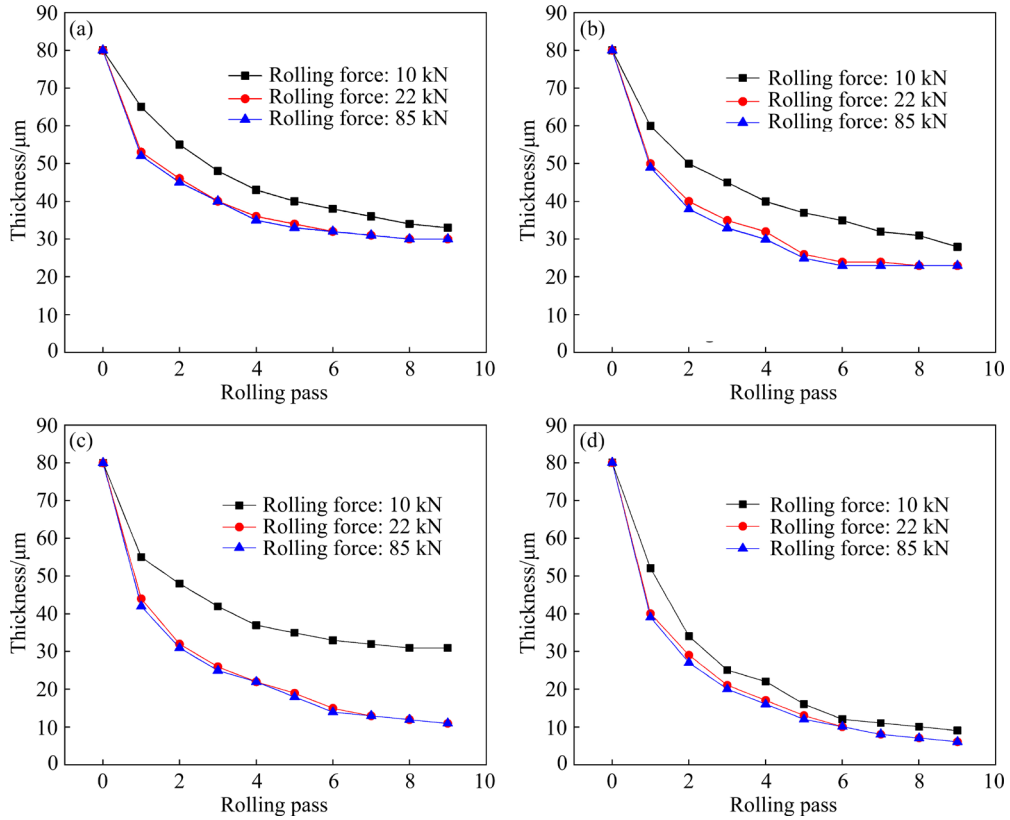

Fig. 4 Relationship between rolling pass and sample thickness at different rolling forces with speed ratios between rolls of 1.0 (a), 1.1 (b), 1.2 (c), and 1.3 (d)

symmetrical and asymmetrical rolling nearly coincide, signifying that a further increase in rolling force does not precipitate a proportional decrease in the thickness of the rolled pieces during the micro-rolling of metal foil. This phenomenon may be ascribed to the elastic deformation of the rolls during the rolling process and the contact between the extremities of the rolls, which precludes the reduction of the roll gap and, consequently, the thickness of the material.

In contrast, when the speed ratio between the rolls is increased from 1.0 (symmetrical rolling) to 1.3 (asymmetrical rolling), a marked reduction in the thickness of the copper foil post-rolling is achieved, irrespective of the rolling force being 10, 22, or 85 kN. This observation suggests that when the desired thinning effect is unattainable through the escalation of rolling force alone, an increase in the speed ratio between rolls can enable further thickness reduction, ultimately approaching the threshold of metal rolling. Asymmetrical rolling thereby achieves thinner foils with lower rolling forces than symmetrical rolling methods.

Figure 5 shows the relationship between the number of rolling passes and sample thickness at varying speed ratios between rolls, with a constant rolling force of 22 kN. In symmetrical rolling, where the speed ratio is maintained at 1.0, it was observed that 30 passes were requisite to achieve a reduction in the thickness of the copper foil from 80 to 21 μm. Conversely, when the speed ratio between rolls was increased to 1.3, the thickness of the copper foil was effectively reduced from 80 to 6 μm

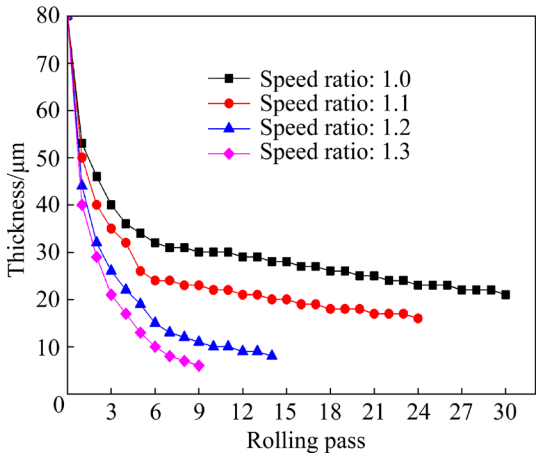

Fig. 5 Relationship between number of rolling passes and sample thickness with rolling force of 22 kN at different speed ratios between rolls

in merely 9 passes. This efficiency is attributed to the disparate linear velocities of the two work rolls during asymmetrical rolling, which induce shear deformation in the rolled piece, thereby facilitating a more pronounced thinning effect. Asymmetrical rolling thus enables the production of thinner foils in a lesser number of passes compared to symmetrical rolling, presenting itself as a cost-effective and efficient technique for the fabrication of metal foils.

3.3 Edge morphologies

Edge morphologies of as-received samples at different rolling reductions in symmetrical rolling are shown in Fig. 6. At a rolling reduction of 68%, micro-cracks were noted to initiate at the edge wave position (Fig. 6(c)), subsequently expanding in a direction forming a 45° angle to the rolling direction (Fig. 6(d)). This orientation of crack propagation is consistent with the direction of shear stress, which is known to be at a 45° angle to the rolling direction [22]. The concentration of stress at the edge region was found to amplify, resulting in an increased number of cracks and a deeper propagation. Traditionally, the emergence of edge cracking has been considered as a sign of the termination of effective plastic deformation. However, it was noted that samples with micro-edge cracks could still undergo further thinning under minimal tensile stress as the rolling reduction was increased (Figs. 6(c) and (d)). Consequently, it is not imperative to equate the initiation of edge cracking with the cessation of effective plastic deformation in the material.

Figure 7 presents the edge morphologies of as-received samples under various reductions in asymmetrical rolling, with the speed ratio of the upper and lower work rolls set at 1.3. Notably, when the reduction is less than 64%, no discernible edge cracking is observed. As deformation progresses, the edge of the copper foil deviates from linearity, and uneven deformation becomes apparent at a reduction of 74%. Micro-edge cracking is observed to initiate at a reduction of 84%. This phenomenon is attributed to the increased work hardening of the copper foil, which leads to a reduction in plasticity, thereby rendering the material more susceptible to edge cracking. It is observed that asymmetrical rolling markedly delays the onset of edge cracking in copper foil compared

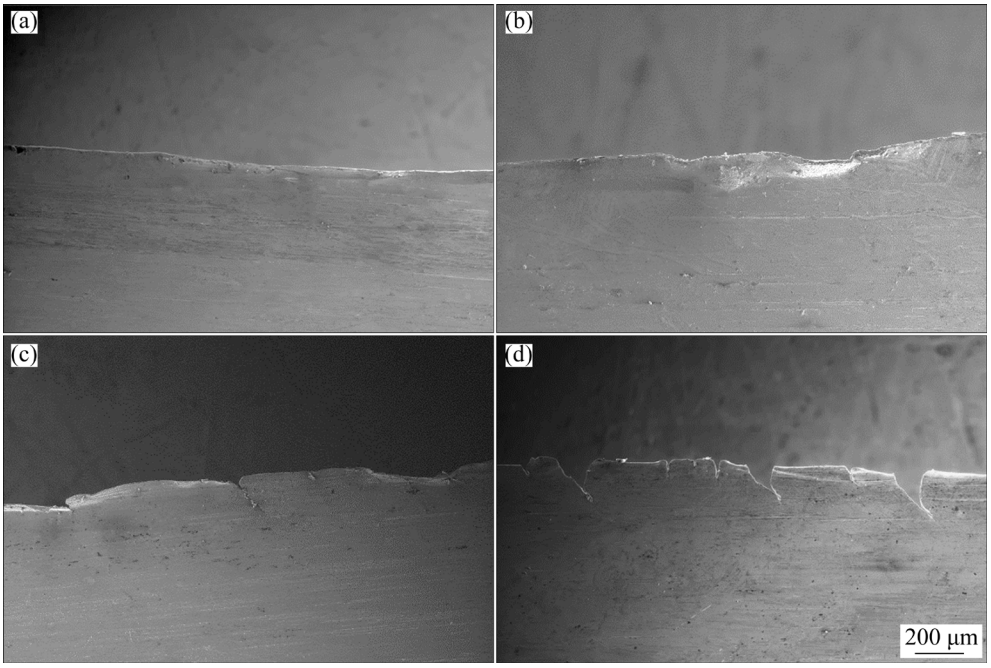

Fig. 6 Edge morphologies of as-received samples at different reductions in symmetrical rolling: (a) 45%; (b) 59%; (c) 68%; (d) 74%

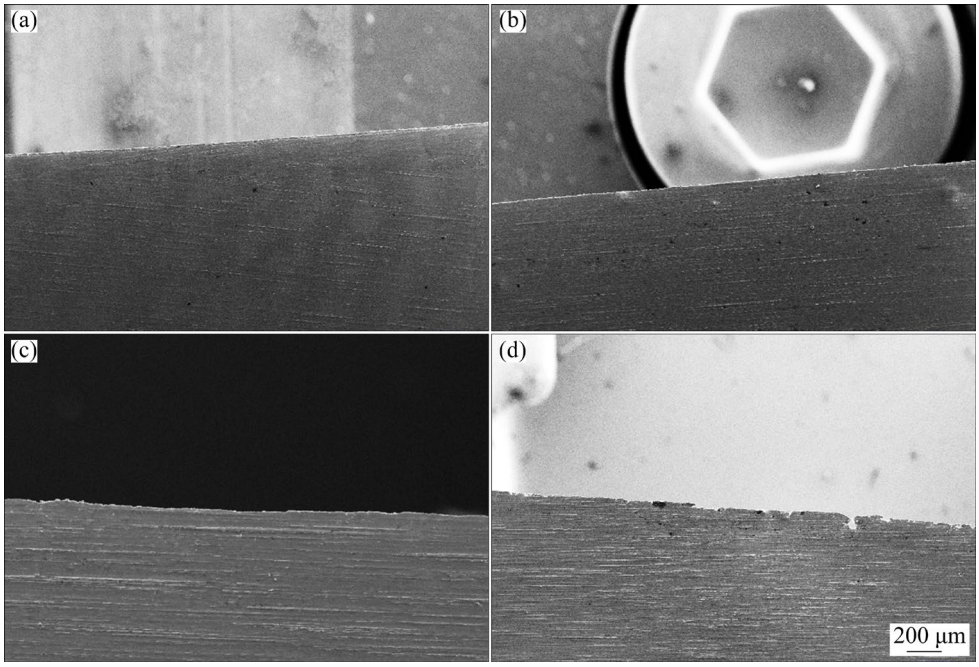

Fig. 7 Edge morphologies of as-received samples with speed ratio between rolls of 1.3 at different reductions in asymmetrical rolling: (a) 50%; (b) 64%; (c) 74%; (d) 84%

to symmetrical rolling, as evidenced by a comparative analysis of Figs. 6 and 7. This finding underscores the advantage of asymmetrical rolling in mitigating edge defects in the micro-rolling process.

Figure 8 shows the edge morphologies of as-received samples at a rolling reduction of 74% with different speed ratios between rolls. When the speed ratio between rolls is 1.0, severe edge cracks are observed to form, with both large and small cracks distributed intermittently throughout the sample. The crack width reaches 100 μm, the depth reaches 200 μm, and the direction of edge crack is gradually 45° from the rolling direction. The presence of such

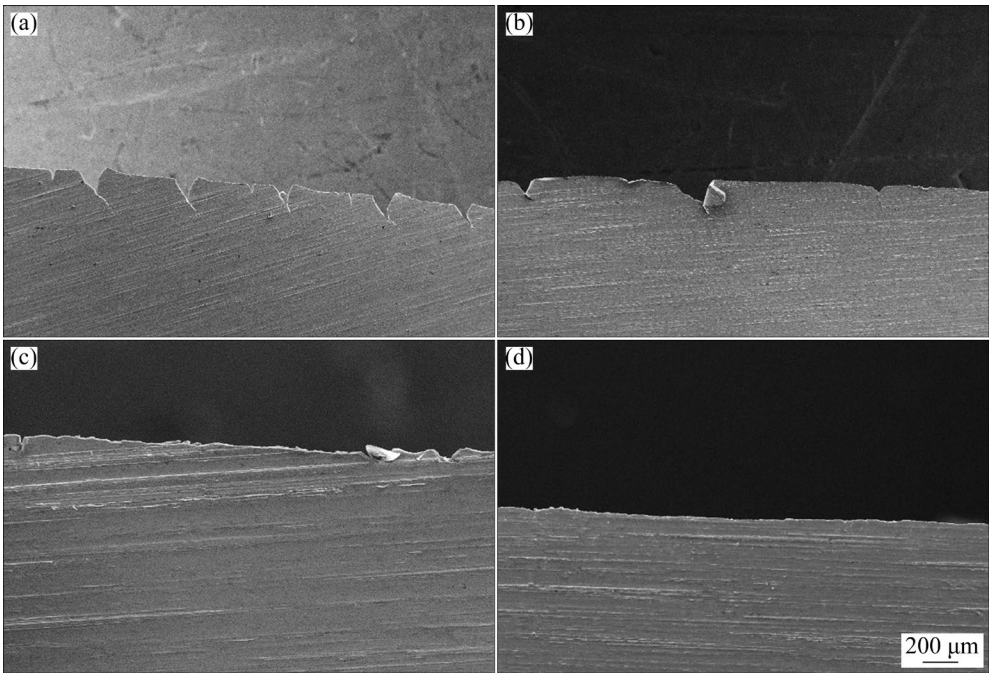

Fig. 8 Edge morphologies of as-received samples at rolling reduction of 74% with different speed ratios between rolls: (a) 1.0; (b) 1.1; (c) 1.2; (d) 1.3

edge cracks poses a significant risk of material failure, potentially leading to the fracture of the rolled piece and consequently halting further processing.

As the speed ratio between rolls gradually increases from 1.0 to 1.3, there is a marked decrease in the incidence and severity of edge crack defects in the copper foil. At a speed ratio of 1.1, the width, depth, and spacing of the cracks are significantly reduced, as depicted in Fig. 8(b). At a speed ratio of 1.2, only a few micro-cracks are visible within the observable field, with the maximum crack width being slightly over 30 μm and the maximum crack depth exceeding 50 μm, as shown in Fig. 8(c). Notably, at a speed ratio of 1.3, the edge cracks are effectively eliminated (Fig. 8(d)).

These findings underscore the efficacy of increasing the speed ratio between rolls in asymmetrical rolling to mitigate edge crack defects in copper foil. The results suggest that optimizing the rolling parameters can significantly enhance the integrity and quality of the rolled material, thereby improving the overall efficiency and effectiveness of the micro-rolling process.

Figure 9 shows edge morphologies of samples at reduction of 84% and speed ratio between rolls of 1.3 with different grain sizes in asymmetrical rolling. The larger the grain size of the rolled piece, the few the number of edge cracks and the deeper the expansion depth, and the larger the spacing between cracks under the same rolling reduction. Coarse-grained samples are more sensitive to edge cracking than fine-grained samples during the rolling process [23]. The initial formation of micro-cracks is often attributed to the transverse expansion of voids located at weak points within the edge region. Grains in the edge region are less constrained compared with internal grains, which makes them more susceptible to stress concentration and uneven deformation in cold rolling. As the grain size increases, the volume fraction of grains in the edge region also rises, exacerbating the degree of uneven deformation in that area. This ultimately leads to the formation of edge cracks upon reaching a critical deformation threshold.

4 Discussion

4.1 Uneven deformation

Cracks occur more readily in the edge region than in the central region, necessitating separate consideration of the edge and central regions when analyzing the causes of edge cracks. Elastic bending

deformation or even contact with each other occurs in two work rolls in the rolling deformation of metal foil (Fig. 10(a)). The distribution of the rolling force (P) along the transverse direction of the rolled piece is characterized by non-uniformity (Fig. 10(b)), with the edge region experiencing a greater rolling force than the central region. This disparity leads to uneven deformation and strain localization, with the latter being identified as the progenitor of edge cracks. Therefore, ensuring the parallelism of the roll gap is essential to mitigate the propensity for edge cracking, considering the sensitivity of edge cracks to the rolling force.

In asymmetrical rolling, the disparate linear velocities of the two work rolls generate shear stress, which plays a crucial role in facilitating the thinning of the rolled pieces and concurrently diminishing the rolling force when compared to symmetrical rolling. An increased speed ratio between the rolls in asymmetrical rolling results in a more pronounced shear stress and a corresponding reduction in rolling force. In this work, the rolling force is reduced from 22 kN in symmetrical rolling to 10 kN in asymmetrical rolling with a speed ratio of 1.3 to obtain the same rolling reduction. This reduction in rolling force in asymmetrical rolling significantly alleviates the elastic flattening and bending deformation of the rolls, as well as the uneven deformation of the rolled piece across the transverse direction. Consequently, asymmetrical rolling is demonstrated to be effective in mitigating edge crack defects when compared to symmetrical rolling at equivalent reductions.

In symmetrical rolling, the friction stress on the surfaces of the backward slip zone is opposite to that in the forward slip zone. The accumulation of

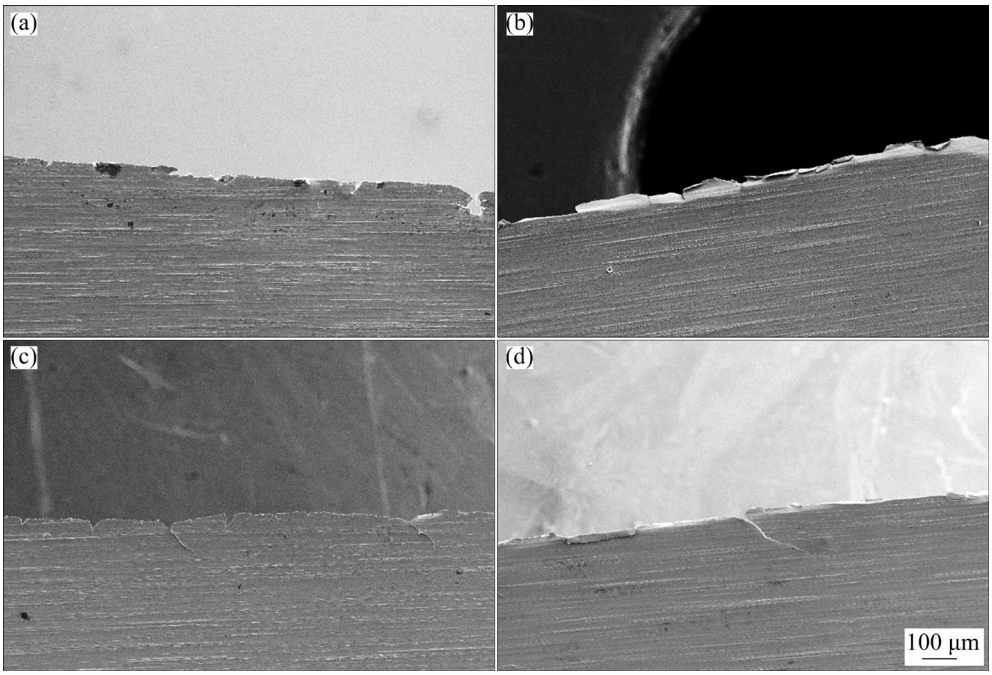

Fig. 9 Edge morphologies of copper foils at reduction of 84% and speed ratio between rolls of 1.3 with different grain sizes: (a) 3.3 μm; (b) 7.7 μm; (c) 23.2 μm; (d) 75.2 μm

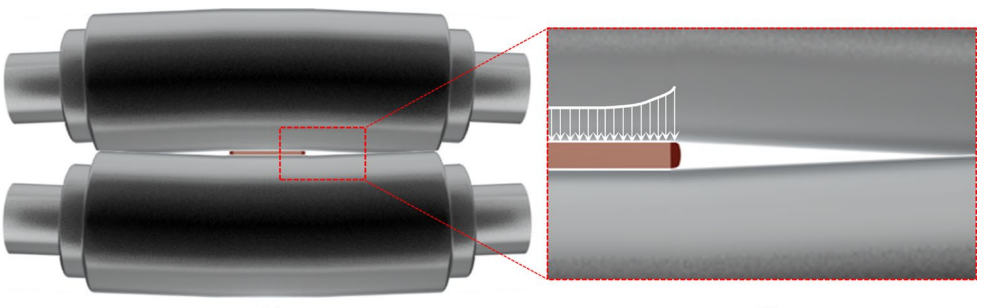

(a) (b)

Fig. 10 Schematic diagrams of roll deformation (a) and rolling force distribution during rolling process (b)

these opposing friction stresses within the two zones contributes to the progressive augmentation of the spherical stress tensor, which is inherently associated with the elastic deformation of the rolled pieces. In contrast, asymmetrical rolling introduces a directional opposition of friction stress on the upper and lower surfaces within the cross-shear zone, thereby intensifying the deviatoric stress tensor. A greater speed ratio between rolls results in a greater cross-shear zone proportion and deviatoric stress tensor, which are reasons for plastic deformation. More prone to plastic deformation resulting in fewer edge crack defects. Asymmetrical rolling achieves superior feasibility for producing high-quality metal foil (with a thickness of less than 100 μm) with few defects than symmetrical rolling.

4.2 Longitudinal secondary tensile stress

Figure 11 presents a schematic representation of the stress states at both the edge and central regions in the rolling deformation zone. During the rolling process, the stress distribution varies along the transverse direction (y-axis) during the rolling process. In the central region of the deformation zone, the metal flow is confined by the surrounding material, resulting in a deformation of zero along the y-axis (ε_{y1}=0). This condition aligns with the requirements for plane strain deformation. Conversely, the metal flow in the edge region is not similarly constrained along the y-axis, leading to non-zero deformation in this direction. As a result, the edge region deviates from the plane strain scenario.

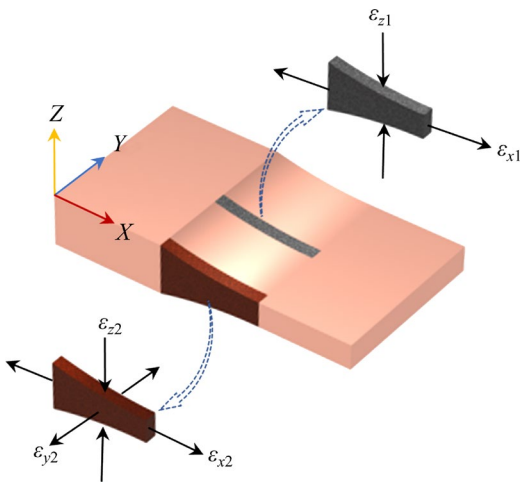

Fig. 11 Schematic diagram of stress states at edge and central regions in rolling deformation zone

Under the assumption of plane upsetting for the rolling process at the edge region, the edge is permitted to deform freely in both the x and y directions, with equal deformation occurring in both directions (ε_{x2}=ε_{y2}). Concurrently, the central region of the metal is considered to deform solely in the x direction, with the center region experiencing twice the deformation in the x direction compared to the edge regions (ε_{x1}=2ε_{x2}). This differential in deformation between the edge and central regions leads to the development of longitudinal secondary tensile stress within the edge region, which is conducive to the initiation of edge cracks.

In asymmetrical rolling, the shear stress in the cross-shear zone promotes the deformation along the x direction (ε_{x2}>ε_{y2}). As a result, the central region deforms in the x direction less than twice the amount of the edge region (ε_{x1}<2ε_{x2}). Consequently, the disparity in deformation between the edge and central regions along the x-axis is minimized. This reduction in deformation disparity is directly associated with a decrease in longitudinal secondary tensile stress, which in turn significantly contributes to a diminished occurrence of edge crack defects.

4.3 Compressive residual stress

The inhomogeneous plastic deformation in rolled pieces caused by the bending deformation of work rolls and other factors in the rolling process can lead to complex residual stresses. In asymmetrical rolling, the unequal linear speed of the two work rolls results in the different deformation degrees of the upper and lower surfaces of rolled pieces, and this uneven deformation induces residual stress in the rolled pieces. Residual stress in metallic materials causes changes in interplanar spacing. Figure 12 shows the relationship between the lattice strain (ε) and the diffraction angle (φ) of the sample in the asymmetrical rolling with different speed ratios between rolls.

The lattice strain (ε) is linearly related to $\sin^2\varphi$, with the slope of the line being m. The residual stress σ_r of the material can be written as

$$\sigma_r = \frac{Em}{1+v} \tag{1}$$

where v and E are the Poisson's ratio and elastic modulus of pure copper, respectively. According to

Eq. (1), the residual stresses of samples are −61.3, −73.5, −94.4 and −116.3 MPa when the speed ratios between rolls are 1.0, 1.1, 1.2 and 1.3, respectively, where the negative sign indicates that the residual stress of copper foil is compressive. The sample with the highest slope at a speed ratio between rolls of 1.3 implies the highest residual compressive stress.

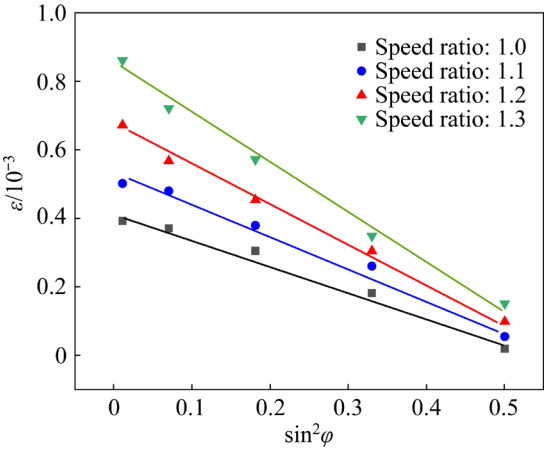

Fig. 12 Relationship between lattice strain and diffraction angle of copper foils in asymmetrical rolling with different speed ratios between rolls

The residual stress distribution in the rolled piece is related to the reduction of the final pass. In micro-rolling, the reduction in the last few passes is very minimal, plastic deformation occurs primarily near the surface layer of the metal material, and with little to no extension in the inner metal. Due to this unequal plastic extension, there must be strain coordination between the surface and the inner layer. The inner material restricts the surface from extending, while the surface material exerts a tensile effect on the inner material. Consequently, the surface layer exhibits residual compressive stress and the inner layer shows residual tensile stress. Furthermore, the shear stress in asymmetrical rolling increases the difference in plastic deformation between the surface and the inner layer in rolled pieces. This enhanced deformation disparity results in a higher level of surface residual compressive stress in asymmetrical rolling compared to symmetrical rolling.

The effect of the surface residual stress on the edge crack can be described by the stress intensity factor (ΔK) of the surface defect in Eq. (2) [9]:

$$\Delta K=0.65(\sigma_m+\sigma_S)\sqrt{\pi\sqrt{A}} \quad (2)$$

where σ_m, σ_S and A correspond to the nominal stress amplitude, surface residual stress and surface defect area, respectively. A smaller ΔK indicates a slower surface crack propagation rate. ΔK increases with the increase of A, so the edge cracks will propagate easily once they form. The surface residual compressive stress increases with the increase of the speed ratio between rolls, which reduces the ΔK of the copper foil, slows down the initiation and propagation of surface cracks [24−26], and significantly reduces the edge crack defects of copper foil.

4.4 Grain size

In Fig. 9, the larger the grain size of the rolled piece, the smaller the number of edge cracks and the deeper the expansion depth, and the larger the spacing between cracks under the same rolling reduction. Polycrystalline materials are considered to be composed of surface and internal parts (Fig. 13(a)) based on the surface layer model (SLM) [27], so the flow stress of the material can be expressed as the sum of the flow stress of the internal and surface grains.

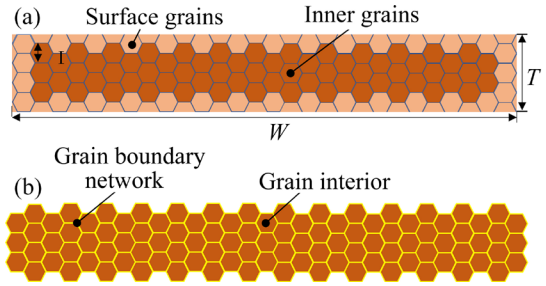

Fig. 13 Schematic diagrams of grain and grain boundary of polycrystalline materials

The flow stress of the material can be expressed as

$$\sigma=f_s\sigma_s+f_i\sigma_i \quad (3)$$

where σ represents the flow stress of the entire material, σ_s and f_s represent the flow stress of the surface grain and the volume fraction of the surface grain in the total grain, respectively, and σ_i and f_i represent the flow stress of the internal grain and the volume fraction of the internal grain in the total grain, respectively. In the forming process of polycrystalline materials (T/D>10), f_s is so small that the effect of surface grain on material properties is considered to be negligible. However, as the scale of the sample diminishes to mesoscopic or microscopic dimensions (T/D<10), the volume

fraction of surface grains within the total grain volume increases. This increase accentuates the impact of surface grains on plastic deformation, making the size effect a critical factor that warrants consideration.

The dislocation distribution within the deformed material differs between the internal and surface regions. In the internal region, dislocations are evenly distributed. In contrast, in the surface region, dislocation entanglement occurs primarily near grain boundary junctions, and a small number of dislocations are distributed within the grains [28]. This phenomenon can be attributed to the minimal constraints imposed by surface grains, which facilitate deformation mechanisms such as grain rotation and grain boundary sliding. These mechanisms result in a reduced flow stress in surface grains. The propensity for edge cracking in copper foil during the rolling process increases with grain size. This trend is due to the escalating proportion of surface grains within the material. During rolling, the coordinated deformation among grains is reduced, leading to a marked reduction in fracture strain as the aspect ratio T/D decreases, particularly when T/D falls below 10. Under these conditions, the influence of longitudinal secondary tensile stress renders the copper foil more susceptible to edge cracking.

Polycrystalline materials can also be considered to be composed of two parts: the grain boundary network and the grain interior [29] (Fig. 13(b)). Therefore, the flow stress of the material can be expressed as the sum of the flow stress of the grain boundary network and grain interior. The flow stress of the material can be expressed as

$$\sigma=f_{gb}\sigma_{gb}+f_{in}\sigma_{in} \quad (4)$$

where σ_{gb} and f_{gb} represent the flow stress and the volume fraction of the grain boundary network in the entire material, respectively, and σ_{in} and f_{in} represent the flow stress and the volume fraction of grain interior in the entire material, respectively.

The dislocation distribution in the grain boundary network and grain interior of deformed materials differs. During the deformation process, the statistically stored dislocations in the grain interior contribute to the work hardening of individual grains. The distribution of geometrically necessary dislocations at the grain boundaries is mainly used to regulate the continuity of plastic strain. The dislocation density at the grain boundaries is higher than that in the grain interior. It has been found that grain boundaries in annealed pure Cu was 1.5 times as hard as that of grain interior [30]. With the increase of grain size, f_{gb} decreases, the barrier effect of grain boundaries on edge cracking is greater than that of grain inner region, the grain boundary hardening effect weakens, the fracture strain of the sample decreases, and the rolling edge crack is easy to occur. A decrease in the T/D ratio exacerbates this tendency by limiting the grain deformation influenced by adjacent grains, thereby accentuating the deformation anisotropy of individual grains. This heightened size effect significantly influences the deformation of copper foil during micro-rolling, increasing the likelihood of edge cracking and other defects.

In fine-grained samples, an abundance of grain boundaries effectively hinders the propagation of initial edge micro-cracks towards the center of the rolled piece. The resistance encountered by the initial crack as it attempts to spread towards the center of the rolled piece exceeds that faced by the edge grain in generating a new crack. Consequently, the number of edge cracks is observed to increase with progressive deformation. In contrast, coarse-grained samples, with their few grain boundaries, exhibit a reduced barrier effect on the growth of edge cracks. Here, the resistance to the initial crack's propagation towards the center of the rolled piece is less than that to the formation of new cracks at the edge, leading to an increased propagation depth of edge cracks with further deformation.

4.5 Slip system

There is a transition from polycrystalline to single-crystal behavior if the value of T/D falls below 10 [21,29], when external forces are applied to polycrystalline materials (T/D>10), the inherent anisotropy of the crystal lattice results in a non-uniform stress distribution across grains of varying orientations. Consequently, the shear stress acting on the slip systems within each grain is markedly different due to the distinct grain orientations. As a result, not all grains initiate deformation simultaneously, grains with favorable orientations begin to slip, while those with unfavorable orientations have yet to engage in

plastic deformation. Moreover, the orientation of the slip system of different orientation grains is also different, so the slip direction is also different, and the slip system cannot be directly extended from one grain to another grain. Each grain is circumscribed by neighboring grains, and its deformation is contingent upon the coordinated deformation of adjacent grains. However, for T/D<10 or even T/D=1, the inter-grain deformation coordination is significantly impaired. This breakdown in coordination is incapable of sustaining the continuity of deformation between grains, which can lead to the formation of micro-cracks and ultimately the rupture of the material.

To coordinate the deformation between the grains in the polycrystalline material, each grain must slip not only on the single slip system with the most favorable orientation but also on several other slip systems, including the slip system with the least favorable orientation, so that its shape can be changed accordingly. Any deformation can be represented by six strain components: ε_{xx}, ε_{yy}, ε_{zz}, and γ_{xy}, γ_{yz} and γ_{xz}, but the crystal volume does not change ($\Delta V/V=\varepsilon_{xx}+\varepsilon_{yy}+\varepsilon_{zz}=0$) during plastic deformation, so there are only five independent strain components, and each independent strain component is generated by an independent slip system. The plastic deformation of polycrystal is to meet the requirements of coordination of grain deformation through the multi-system slip of each grain. The plastic deformation of polycrystals requires that each grain can be able to slip on at least five independent slip systems. However, considering the extreme case in this study (T/D=1.1), it is pertinent to investigate whether an adequate number of slip systems are available to facilitate metal deformation during the rolling process. In such instances, the deformation behavior of individual grains significantly influences the overall deformation characteristics of the copper foil. Examining the initiation and cessation of slip systems in this type of copper foil provides a clear understanding of the plastic deformation capabilities of metal grains during both symmetrical and asymmetrical rolling processes.

In our previous work, crystal plasticity finite element simulation was carried out to compare the start-stop states of the slip system at specific locations of copper foil with T/D=1 during symmetrical and asymmetrical rolling [31]. In the surface region of the grain, there are six slip systems $(111)[10\bar{1}]$, $(111)[\bar{1}10]$, $(\bar{1}11)[110]$, $(\bar{1}11)[0\bar{1}1]$, $(1\bar{1}1)[011]$ and $(1\bar{1}1)[10\bar{1}]$ activated by sliding deformation in symmetrical and asymmetrical rolling. The sliding laws of the six starting slip systems are similar. However, in the central region of the grain, a total of seven slip systems are activated in symmetrical rolling while nine slip systems are activated in asymmetrical rolling, where $(1\bar{1}1)[110]$ and $(11\bar{1})[101]$ are new starting slip systems. Slip systems $(111)[10\bar{1}]$, $(\bar{1}11)[0\bar{1}1]$ and $(11\bar{1})[\bar{1}10]$ have stronger slip and $(11\bar{1})[\bar{1}10]$ sliding state changes intenser in asymmetrical rolling. Therefore, even under the extreme condition of T/D=1, an adequate number of slip systems are activated during sample rolling deformation to ensure the basic plastic deformation of the material. Asymmetrical rolling has the capacity to activate a greater number of slip systems compared to symmetrical rolling, allowing for a more diverse spatial orientation during sliding. This increased activation is instrumental in enabling the rolled piece to circumvent edge crack defects, even under conditions of significant plastic deformation.

5 Conclusions

(1) Sharp reduction of plasticity of rolled pieces caused by work hardening, uneven deformation and longitudinal secondary tensile stress in the edge region of rolled pieces during rolling lead to the initiation of edge cracks, and the crack propagation direction is 45° from the rolling direction.

(2) Asymmetrical rolling can effectively reduce edge crack defects. The reduction in the onset of edge cracks increased from 68% in symmetrical rolling to 84% in asymmetrical rolling. This is mainly because asymmetrical rolling can effectively reduce rolling force, thus reducing elastic bending of rolls and uneven deformation at the edge region of rolled pieces. The shear stress in the cross-shear zone promotes longitudinal deformation and reduces the longitudinal secondary tensile stress at the edge of the rolled piece.

(3) The surface residual compressive stress of copper foil in asymmetrical rolling with a speed ratio between rolls of 1.3 is approximately twice that of symmetrical rolling. The residual

compressive stress generated by the uneven deformation reduces the ΔK and slows the initiation and expansion of surface cracks, thus effectively reducing the edge-cracking defects in copper foil.

(4) The size effect on the deformation of copper foil becomes particularly pronounced when the T/D ratio falls below 10. Under such conditions, both the fracture stress and fracture strain are significantly reduced, making the material more prone to defects, including edge cracks, during the rolling deformation process. The larger the grain size of the rolled piece, the smaller the number of edge cracks and the deeper the expansion depth, and the larger the spacing between cracks under the same rolling reduction.

CRediT authorship contribution statement

Jing-qi CHEN: Conceptualization, Methodology, Resources, Writing − Original draft, Writing − Review & editing, Funding acquisition; **Lin-yun ZHENG** and **Wei ZHAO:** Investigation, Writing − Review & editing, Funding acquisition; **Zhen-hua BAI** and **Xue-tong LI:** Writing − Review & editing, Supervision; **Ri-huan LU** and **Shou-dong CHEN:** Investigation, Data curation, Funding acquisition; **Xiang-hua LIU:** Writing − Review & editing, Supervision; **Hai-tao GAO:** Investigation, Data curation, Funding acquisition; **Hai-liang YU:** Conceptualization, Methodology, Resources, Writing − Original draft, Writing − Review & editing, Funding acquisition.

Declaration of competing interest

The authors declare that they have no known competing financial interests or personal relationships that could have appeared to influence the work reported in this paper.

Acknowledgments

This study was supported by the National Natural Science Foundation of China (Nos. 52204401, 52005432), Hebei Natural Science Foundation of China (No. E2021203179), Excellent Young Talents Program of University of Anhui Province, China (No. gxyq2022093), and Excellent Youth Research Projects in Universities of Anhui Province, China (No. 2022AH030153).

References

[1] YANG Guang, HUI Yue, CHEN Ju, LI Bo, CHEN Jian-hua, LIU Kai, LIANG Gui-de, DENG Ding-rong. Effect of discrete Cr nano-nuclei on stripping property and resistivity of ultrathin Cu foil [J]. Transactions of Nonferrous Metals Society of China, 2023 33(9): 2698−2711.

[2] ZHANG Yan-qiu, JIANG Shu-yong. Molecular dynamics simulation on mechanisms of plastic anisotropy in nanotwinned polycrystalline copper with {111} texture during tensile deformation [J]. Transactions of Nonferrous Metals Society of China, 2021, 31(5): 1381−1396.

[3] WAN Shan, LIAO Bo-kai, DONG Ze-hua, GUO Xing-peng. Comparative investigation on copper atmospheric corrosion by electrochemical impedance and electrical resistance sensors [J]. Transactions of Nonferrous Metals Society of China, 2021, 31(10): 3024−3038.

[4] YAN Yu-xi, SUN Qu-an, CHEN Jian-jun, PAN Hong-liang. Effect of processing parameters on edge cracking in cold rolling [J]. Materials and Manufacturing Processes, 2013, 30(10): 1174−1178.

[5] XIE H B, JIANG Z Y, YUEN W Y D. Analysis of friction and surface roughness effects on edge crack evolution of thin strip during cold rolling [J]. Tribology International, 2011, 44(9): 971−979.

[6] ZHANG Ding-fei, DAI Qing-wei, FANG Lin, XU Xing-xing. Prediction of edge cracks and plastic-damage analysis of Mg alloy sheet in rolling [J]. Transactions of Nonferrous Metals Society of China, 2011, 21(5): 1112−1117.

[7] AN Hong-ya, GAO Peng, CHU Xiao-feng, WANG Jian, PENG Xin-yu. Study on the mechanism of edge cracking in cold rolled silicon steel [J]. Metallurgy and Materials, 2023, 43(3): 43−45.

[8] IKUMAPAYI O M, AKINLABI E T, ONU P, ABOLUSORO O P. Rolling operation in metal forming: Process and principles—A brief study [J]. Materials Today: Proceedings, 2020, 26: 1644−1649.

[9] LEE S H, LEE K H, LEE S B, KIM B M. Study of edge-cracking characteristics during thin-foil rolling of Cu−Fe−P strip [J]. International Journal of Precision Engineering and Manufacturing, 2013, 14(12): 2109−2118.

[10] WANG Xi-yong, LIU Xue-feng, SHI Lai-xin, LI Jing-kun, XIE Jian-xin. Characteristic and formation mechanism of Matt surface of double-rolled copper foil [J]. Journal of Materials Processing Technology, 2015, 216: 463−471.

[11] CHEN Shou-dong, LIU Xiang-hua, LIU Li-zhong. Effects of grain size and heterogeneity on the mechanical behavior of foil rolling [J]. International Journal of Mechanical Sciences, 2015, 100: 226−236.

[12] SOMEKAWA H, MOTOHASHI N, KURODA S, MANDAI T. Mechanical and functional properties of ultra-thin Mg foils [J]. Materials Science and Engineering: A, 2023, 872: 144934.

[13] ZHAO Jing-wei, HUO Ming-shuai, MA Xiao-guang, JIA Fang-hui, JIANG Zheng-yi. Study on edge cracking of copper foils in micro rolling [J]. Materials Science and Engineering: A, 2019, 747: 53−62.

[14] WANG Ji, LIU Xiang-hua, GUO Wang-peng. Analysis of mechanical parameters for asymmetrical strip rolling by slab method [J]. The International Journal of Advanced Manufacturing Technology, 2018, 98(9/10/11/12): 2297−2309.

[15] TANG De-lin, LIU Xiang-hua, LI Xiang-yu, PENG Liang-gui. Permissible minimum thickness in asymmetrical cold rolling [J]. Journal of Iron and Steel Research International, 2013, 20(11): 21−26.

[16] TANG De-lin, LIU Xiang-hua, SONG Meng, YU Hai-liang. Experimental and theoretical study on minimum achievable foil thickness during asymmetric rolling [J]. Plos One, 2014, 9(9): e106637.
[17] CHEN Jing-qi, ZHAO Yang, GAO Hai-tao, CHEN Shou-dong, LI Wen-Jin, LIU Xiang-hua, HU Xian-lei, YAN Shu. Rolled electrodeposited copper foil with modified surface morphology as anode current collector for high corrosion resistance in lithium-ion battery electrolyte [J]. Surface and Coatings Technology, 2021, 421: 127369.
[18] CHEN Jing-qi, WANG Xiao-gong, GAO Hai-tao, YAN Shu, CHEN Shou-dong, LIU Xiang-hua, HU Xian-lei. Rolled electrodeposited copper foil with modified surface morphology as anode current collector for high performance lithium-ion batteries [J]. Surface and Coatings Technology, 2021, 410: 126881.
[19] ASTM E8/E8M—21. Standard Test Methods for Tension Testing of Metallic Materials [S]. West Conshohocken, PA: ASTM International, 2021.
[20] CHEN Jing-qi, GAO Hai-tao, HU Xian-lei, YANG Liu-qing, KE Di-wen, LIU Xiang-hua, YAN Shu, LU Ri-huan, MISRA R D K. The significant size effect on nucleation and propagation of crack during tensile deformation of copper foil: Free surface roughening and crystallography study [J]. Materials Science and Engineering: A 2020, 790: 139678.
[21] VOLLERTSEN F, SCHULZE NIEHDFF H, HU Z. State of the art in micro forming [J]. International Journal of Machine Tools and Manufacture, 2006, 46(11): 1172−1179.
[22] XIE Hai-bo, JIANG Zheng-yi, WEI Dong-bin, TIEU A K. Analysis of edge crack of thin strip during cold rolling [J]. Materials Science Forum, 2010, 654/655/656: 222−225.
[23] DODD B, BODDINGTON P. The causes of edge cracking in cold rolling [J]. Journal of Mechanical Working Technology, 1980, 3(3/4): 239−252.
[24] LU J Z, LUO K Y, YANG D K, CHENG X N, HU J L, DAI F Z, QI H, ZHANG L, ZHONG J S, WANG Q W, ZHANG Y K. Effects of laser peening on stress corrosion cracking (SCC) of ANSI 304 austenitic stainless steel [J]. Corrosion Science, 2012, 60: 145−152.
[25] SANO Y, OBATA M, KUBO T, MUKAI N, YODA M, MASAKI K, OCHI Y. Retardation of crack initiation and growth in austenitic stainless steels by laser peening without protective coating [J]. Materials Science and Engineering: A, 2006, 417(1/2): 334−340.
[26] LUONG H, HILL M R. The effects of laser peening on high-cycle fatigue in 7085-T7651 aluminum alloy [J]. Materials Science and Engineering: A, 2008, 477(1/2): 208−216.
[27] RAN J Q, FU M W, CHAN W L. The influence of size effect on the ductile fracture in micro-scaled plastic deformation [J]. International Journal of Plasticity, 2013, 41: 65−81.
[28] MIYAZAKI S, SHIBATA K, FUJITA H. Effect of specimen thickness on mechanical properties of polycrystalline aggregates with various grain sizes [J]. Acta Metallurgica, 1979, 27(5): 855−862.
[29] FU M W, CHAN W L. Geometry and grain size effects on the fracture behavior of sheet metal in micro-scale plastic deformation [J]. Materials & Design, 2011, 32(10): 4738−4746.
[30] SOIFER Y M, VERDYAN A, KAZAKEVICH M, RABKIN E. Nanohardness of copper in the vicinity of grain boundaries [J]. Scripta Materialia, 2002, 47(12): 799−804.
[31] CHEN Shou-dong, CHEN Jing-qi, LI Jie, SUN Jian, LU Ri-huan. Prediction of deformation localization of copper foil compound forming rolling using crystal plasticity finite element simulations [J]. Materials Reports, 2023, 37(2): 21050240.

异步微轧制中铜箔的边裂行为

陈敬琪[1,2]，郑淋匀[1,2]，赵 威[1,2]，白振华[1,2]，
李学通[1,2]，卢日环[1,2]，陈守东[3]，刘相华[4]，高海涛[5]，喻海良[5]

1. 燕山大学 国家冷轧板带装备及工艺工程技术研究中心，秦皇岛 066004；
2. 燕山大学 机械工程学院，秦皇岛 066004；
3. 铜陵大学 机械工程学院，铜陵 244061；
4. 东北大学 材料科学与工程学院，沈阳 110819；
5. 中南大学 机电工程学院，长沙 410083

摘 要：研究铜箔在异步微轧制过程中的边裂行为，分析异步轧制中异速比、晶粒尺寸和变形区应力状态对边缘裂纹的影响。轧制过程中被轧件边缘区域的塑性低、变形不均匀以及纵向二次拉应力是产生边裂的主要原因。轧制件的晶粒尺寸越大，在相同的压下率时，边缘裂纹深度越深，裂纹间距越大，裂纹数量越少。相比于同步轧制，异步轧制可以有效提高铜箔出现边裂的压下率，这是因为异步轧制可以产生剪切应力，降低轧制力和纵向二次拉应力，增加表面残余压应力。增加异步轧制的异速比可以有效地减少铜箔的边裂缺陷。

关键词：边裂；铜箔；异步轧制；尺寸效应

(Edited by Xiang-qun LI)